Chapter 2

Theoretical Framework for Terahertz Measurement

This chapter is concerned with basic concepts and theories that form the foundation for understanding the unique characteristics of terahertz (THz) radiation. We begin the chapter with interactions of electromagnetic wave with matter, which give rise to derivation of propagation and transfer matrices of electric fields through dielectric media. Thereafter, spectral reflectance of THz response on proton exchange membrane (PEM) fuel cell structure is formulated. The theoretical calculation will ensure capability to identify water in the PEM fuel cell of THz imaging. Finally, we end the chapter with a frequency filtering method using a metal mesh, which will be exploited to improve spatial resolution in THz imaging measurement.

2.1 Interactions of Electromagnetic Wave with Matter

Illustrated in Figure 2.1 are interactions of electromagnetic wave with matter. We will describe briefly of the three phenomena: absorption, reflection and refraction.

2.1.1 Absorption

Absorption is the way that electromagnetic waves loss energies during wave propagation in matters. Absorption coefficient is a way to determine how quickly and effectively radiation is absorbed in a certain medium. The absorption of light during

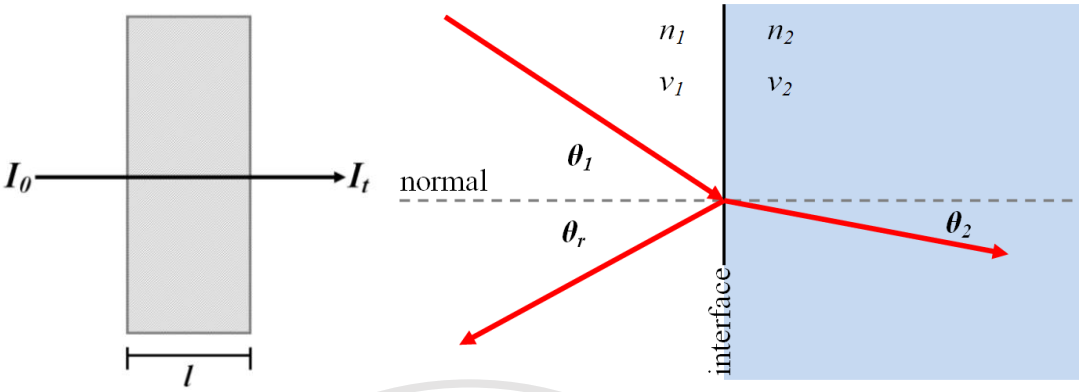

Figure 2.1: Interactions of light with medium *via* (a) absorption, (b) reflection and refraction

wave propagation is often called attenuation. The absorption of electromagnetic radiation by a medium results in a loss of transmitted intensity which is exponential with depth into a material. The Beer-Lambert law is used to describe the absorption of photons in a non-scattering medium. For uniformly absorbing medium, this law states that the product of absorption coefficient by the distance the light travels through the medium (α known as the absorption coefficient of the medium) is equal to the log_{10} of the ratio of the light intensity incident on the medium, I_0, and the light intensity passed through the medium, I_t, as written in Equation 2.1:

$$\alpha \cdot l = log_{10} \frac{I_0}{I_t} \tag{2.1}$$

2.1.2 Reflection

Reflection is the change in direction of a wave front at an interface between two different media so that the wave front returns into the medium from which it originated. It occurs on almost all surfaces: some reflect a major fraction of the incident light, while others reflect only a part of it, and absorb the rest. When a wave approaches a reflecting surface, such as a mirror, the wave that strikes the surface is called the incident wave, and the one that bounces back is called the reflected wave. An imaginary line perpendicular to the surface at the point at which the incident wave

strikes is called the normal. The angle between the incident wave and the normal is called the angle of incidence. The angle between the reflected wave and the normal is called the angle of reflection. Reflection of light from surface is also governed by the two laws of reflection:

1. The incident wave, reflected wave and the normal at the point of incidence lie on the same plane.

2. The angle of incidence is equal to the angle of reflection.

2.1.3 Refraction

Refraction is the bending of a wave due to a change in its speed. This is the most commonly observed when the wave passes from one medium to another at any angle other than 90 or 0 degree. The amount of bending depends on the indices of refraction of the two media which are defined as the speed of light in vacuum divided by the speed of light in the media and is also described quantitatively by Snell's law. Snell's law relates the indices of refraction, *n*, of the two media to the direction of propagation in term of angle to the normal, as shown in Equation 2.2:

$$\frac{\theta_1}{\theta_2} = \frac{v_1}{v_2} = \frac{n_2}{n_1} \tag{2.2}$$

where θ_1 is the angle of incidence and θ_2 is the angle of refraction, and n_1 and n_2 are the indices of refraction, and v_1 and v_2 are the wave velocities in the respective media.

If the incident medium has index of refraction larger than that of the refraction medium, then the angle with the normal is increased by refraction. On the other hand, if the refraction medium has index of refraction larger than that of incident medium then the angle with the normal is decreased.

2.2 Matrix of Light Transport

In this section we want to derive the transfer and propagation matrices for an electromagnetic wave traveling through medium. The combination of a transfer and a propagation matrix relating the fields across different interfaces will be referred to as

a transition matrix. From the elementary laws of geometric optics we know that part of the wave is reflected and part of the wave is refracted. Furthermore, both *E* and *H* obey the boundary conditions that the tangential components of the vector fields are continuous across the interface. The distinct media are denoted by the indices 1 and 2, i.e.,

$$E_1 = E_2 \quad , \quad H_1 = H_2 \tag{2.3}$$

We also define the intrinsic impedance, η, of a material to be the ratio of the electric to magnetic field amplitudes. A relationship that we will use extensively in this presentation is

$$\eta = \frac{E}{H} = \sqrt{\frac{\mu}{\epsilon}} = \sqrt{\frac{\mu_0}{\epsilon_0}\frac{\mu_r}{\epsilon_r}} = \eta_0 \frac{\mu_r}{n} = \eta_0 \frac{n}{\epsilon_r} \tag{2.4}$$

where ϵ_r is the relative permittivity, μ_r is the relative permeability and n is the refractive index of material. η_0 is the intrinsic impedance of vacumm. For a non magnetic material, we have $\mu = \mu_0$ or $\mu_r = 1$ and the characteristic impedance become simply $\eta = \eta_0/n$.

2.2.1 Propagation matrix

We start by discussing the propagation matrices. Consider an electric field that is linearly polarized in the *x* direction and propagating along the *z* direction in a homogeneous and isotropic medium [13]. Setting $\boldsymbol{E}(z) = \hat{x}E(z)$ and $\boldsymbol{H}(z) = \hat{y}H(z)$, we have

$$E(z) = E_{0+}e^{i(\omega t - kz)} + E_{0-}e^{i(\omega t + kz)} = E_+(z) + E_-(z) \tag{2.5}$$

$$H(z) = \frac{1}{\eta}[E_{0+}e^{i(\omega t - kz)} - E_{0-}e^{i(\omega t + kz)}] = \frac{1}{\eta}[E_+(z) + E_-(z)] \tag{2.6}$$

where E_{0+} , E_{0-} correspond to forward and backward electric fields at position $z = 0$

Figure 2.2 depicts the quantities $\{E_+(z), E_-(z)\}$ at the two locations z_1 and z_2 separated by a distance $l = z_2 - z_1$. Using Equation 2.5 for the forward field at these two positions, we have

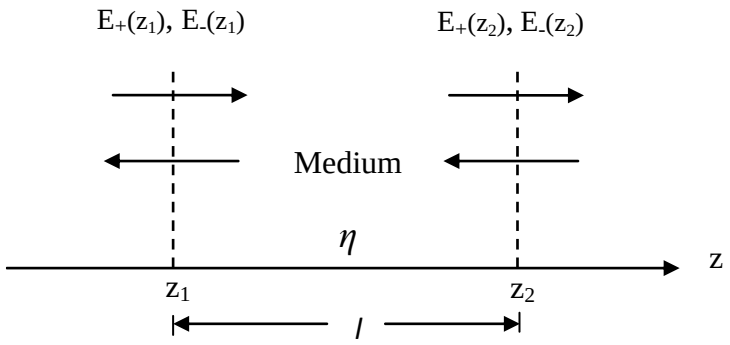

Figure 2.2: Electric field propagated between two positions in space.

$$E_+(z_1) = E_{0+}e^{i(\omega t - kz_1)} \tag{2.7}$$

$$E_+(z_2) = E_{0+}e^{i(\omega t - kz_2)} = E_{0+}e^{i[wt - k(z_1+l)]} = e^{-ikl}E_+(z_1) \tag{2.8}$$

Similarly, $E_-(z_2) = e^{ikl}E_-(z_1)$. Thus, we can write $E_+(z_2)$ and $E_-(z_2)$ in a matrix form as follows:

$$\begin{bmatrix} E_+(z_2) \\ E_-(z_2) \end{bmatrix} = \begin{bmatrix} e^{-ikl} & 0 \\ 0 & e^{ikl} \end{bmatrix} \begin{bmatrix} E_+(z_1) \\ E_-(z_1) \end{bmatrix} \tag{2.9}$$

$$\underline{P} = \begin{bmatrix} e^{-ikl} & 0 \\ 0 & e^{ikl} \end{bmatrix} \tag{2.10}$$

The propagation matrix, $\underline{P}$, describes the behavior of the electric field as it travels through a material. For the propagation of a wave across a length *l*, the transmitted electric field is the incident field attenuated by a factor of e^{-ikl}.

2.2.2 Transfer matrix

Next, we consider a problem of a plane wave normally incident on a planar interface separating two linear media with different optical properties. We will assume that the media are not ferromagnetic and have a permeability, permittivity and refractive index, as show in Figure 2.3 [14].

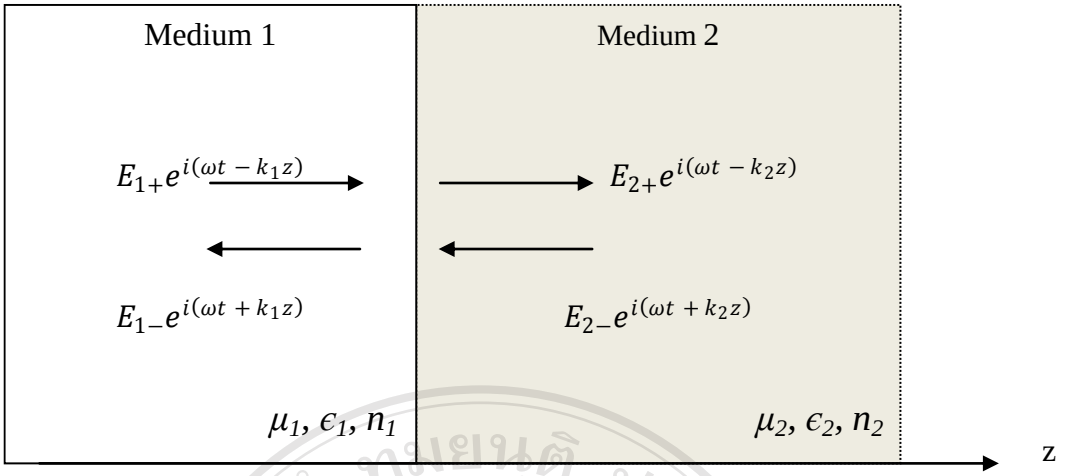

Figure 2.3: Field across an interface.

It is conventional to define electric field that is linearly polarized in the *x*-direction and propagation along the *z*-direction in the media. The forward and backward waves in medium 1 can be expressed in the form show in Equations 2.11 and 2.12.

$$\boldsymbol{E}_1(z) = (E_{1+}e^{i(\omega t - k_1 z)} + E_{1-}e^{i(\omega t + k_1 z)})\hat{x} \tag{2.11}$$

$$\boldsymbol{H}_1(z) = \frac{1}{\eta_1}(E_{1+}e^{i(\omega t - k_1 z)} - E_{1-}e^{i(\omega t + k_1 z)})\hat{y} \tag{2.12}$$

Likewise, the forward and backward waves in medium 2 take the form given by Equation 2.13 and 2.14 change indices of *k* and η.

$$\boldsymbol{E}_2(z) = (E_{2+}e^{i(\omega t - k_2 z)} + E_{2-}e^{i(\omega t + k_2 z)})\hat{x} \tag{2.13}$$

$$\boldsymbol{H}_2(z) = \frac{1}{\eta_2}(E_{2+}e^{i(\omega t - k_2 z)} - E_{2-}e^{i(\omega t + k_2 z)})\hat{y} \tag{2.14}$$

We can now write the boundary condition by using Equation 2.3, at the interface. The requirements of the boundary conditions are that the tangential components of the total vectors ***E*** and ***H*** on two sides of the interface must be the same. In term of the forward and backward electric fields,

$$E_{1+} + E_{1-} = E_{2+} + E_{2-} \tag{2.15}$$

$$\frac{1}{\eta_1}(E_{1+} - E_{1-}) = \frac{1}{\eta_2}(E_{2+} - E_{2-}) \tag{2.16}$$

Equation 2.15-2.16 may be written in the convenient matrix form relating the fields $E_{2\pm}$ on the left of the interface to the fields $E_{1\pm}$ on the right:

$$\begin{bmatrix} E_{2+} \\ E_{2-} \end{bmatrix} = \frac{1}{\tau}\begin{bmatrix} 1 & \rho \\ \rho & 1 \end{bmatrix}\begin{bmatrix} E_{1+} \\ E_{1-} \end{bmatrix} \tag{2.17}$$

where ρ, τ is the elementary reflection and transmission coefficients from the left side of the interface defined in term of intrinsic impedance or the refractive indices as follow:

$$\rho = \frac{\eta_1 - \eta_2}{\eta_2 + \eta_1} = \frac{n_2 - n_1}{n_1 + n_2} \tag{2.18}$$

$$\tau = \frac{2\eta_1}{\eta_1 + \eta_2} = \frac{2n_2}{n_1 + n_2} \tag{2.19}$$

The Transfer matrix, $\underline{T}$, i.e,

$$\underline{T} = \frac{1}{\tau}\begin{bmatrix} 1 & \rho \\ \rho & 1 \end{bmatrix} \tag{2.20}$$

describes the behavior of the electric and magnetic fields ***E, H*** as it across the interface.

2.3 Terahertz Response of Proton Exchange Membrane Fuel Cell Structures

We will use the light transport matrices, introduced in section 2.2, to calculate reflection of THz signal from the PEM fuel cell designed in Chapter 1. Since the structure of fuel cell is multilayer, we illustrate its cross section at the cathode side of the fuel cell as shown in Figure 2.4. As point out in the Figure, the incident THz wave strikes the PEM fuel cell at two different regions: one is the rib region, and the other one is the flow channel region.

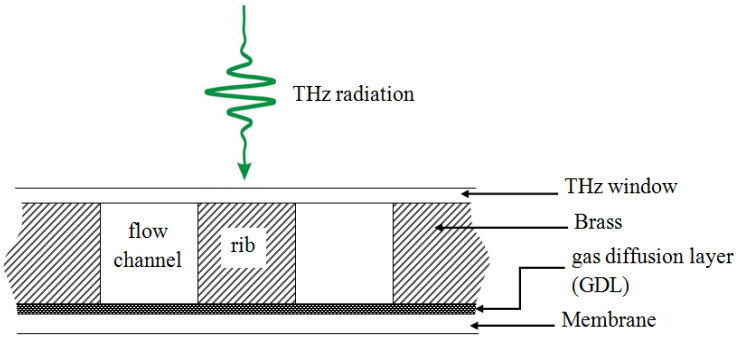

Figure 2.4: Schematic diagram of a cross section of PEM fuel cell structure at the cathode.

Calculation of reflection is therefore a multiple interface problems, which can be handled in a straight forward way with the help of the transfer and propagation matrices. In Figure 2.5, the incident signal, E_{1+}, and the reflectance signal, E_{1-}, are measured experimentally. The incident and reflected fields are considered at the left of each interface. If we wish to determine the overall reflection response, $\Gamma_1 = E_{1-}/E_{1+}$, then we must work with the matrix formulation, starting at the left interface and successively applying the transfer and propagation matrices.

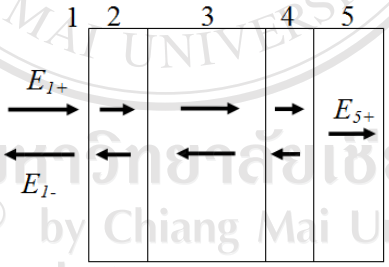

Figure 2.5: Forward and backward electric fields at multistructure of the fuel cell.

As a result, we obtain

$$\begin{bmatrix} E_{5+} \\ 0 \end{bmatrix} = T_4 P_4 T_3 P_3 T_2 P_2 T_1 \begin{bmatrix} E_{1+} \\ E_{1-} \end{bmatrix} \tag{2.21}$$

$$\Gamma_j = \frac{\rho_j + \Gamma_{j+1} e^{-2ik_{j+1}l_{j+1}}}{1 + \rho_j \Gamma_{j+1} e^{-2ik_{j+1}l_{j+1}}} \tag{2.22}$$

when j = 1, 2, 3, 4, and $\Gamma_4 = \rho_4$

This calculation requires two parameters to be set before analysis: the elementary reflection ($\rho_j = \frac{n_{j+1} - n_j}{n_j + n_{j+1}}$), and the phase thickness ($k_j l_j = \frac{2\pi(n_j l_j)}{\lambda}$). Where *n* is a refractive index of each layer indicated by subscription, and *l* is the thickness of matter. Refractive indices of layers which are components in the structure of fuel cell are listed in Table 2.1.

Table 2.1: Reflective indices of materials in multilayer of PEM fuel cell at THz region [15 - 17].

Materials	Refractive index	Thickness (mm)
Air	1.000	-
Silicon	3.416	0.25
PMMA	1.461	1.00
Water	2.098	2.00
Graphite (GDL)	22.713	0.35
Brass	335.158	2.00
Oxygen	0.998	2.00
Nafion membrane	1.380	0.18

The radiation spectral reflection from multiple interfaces of the PEM fuel cell is also has frequency dependence. Calculations of reflected signal with respect to wavenumber from multilayer structures of each window type (poly-methyl-methacrylate (PMMA), silicon (Si) windows) are plotted in Figure 2.6 – 2.7. The results cannot be distinguished clearly between the flow channel with and without water due to the complicate PEM fuel cell structure.

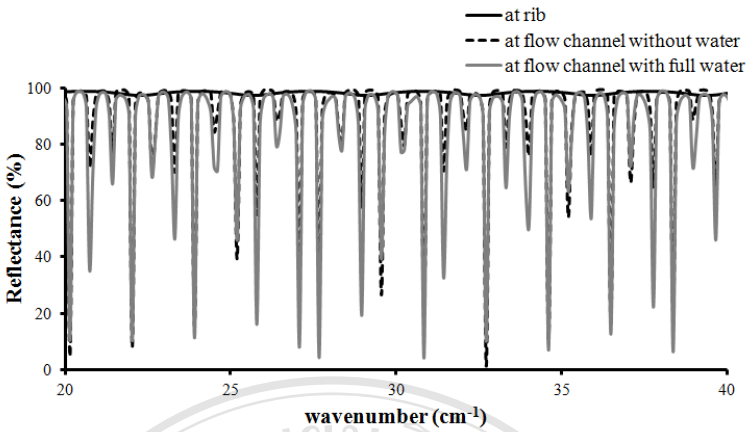

Figure 2.6: Spectral reflectance of the PEM fuel cell structure with PMMA window.

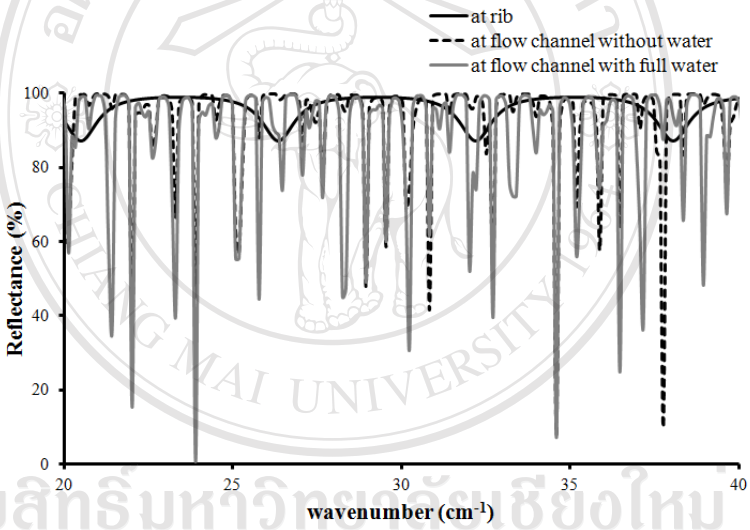

Figure 2.7: Spectral reflectance of the PEM fuel cell structure with Si window.

Hence convenient for this work, we consider the PEM fuel cell only three layers. We define the multilayer by the order from top to bottom of the layer. For example, we call the multilayer in Figure 2.8(left) air|Si|water, and for Figure 2.8(right), we call the multilayer air|Si|air.

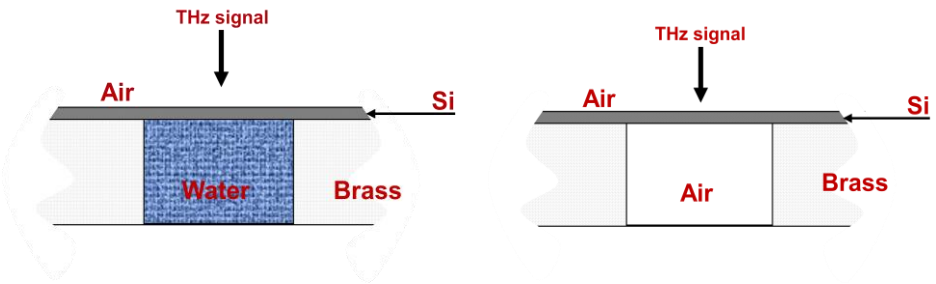

Figure 2.8: Schematic diagram of a cross section of PEM fuel cell structure with filled water, called air|Si|water (left), and unfilled water, called air|Si|air (right).

Calculations of reflected signal with respect to wavenumber from multilayer structures of each window type are plotted in Figure 2.9 and 2.11. We found that the signals of both types of window without water in the channel are noticeably higher than that of those with water. The results suggest that we should be able to identify water in the channel from both types of window. Furthermore, we compare the reflection signal from Si window with water in the channel to PMMA window, i.e., the signal of air|Si|water to air|PMMA|water (Figure 2.11). We found that the reflectance of air|Si|water yields much higher signal than that of air|PMMA|water. The calculation results suggest that we should be able to detect presence of water in the flow channels *via* reflective THz imaging.

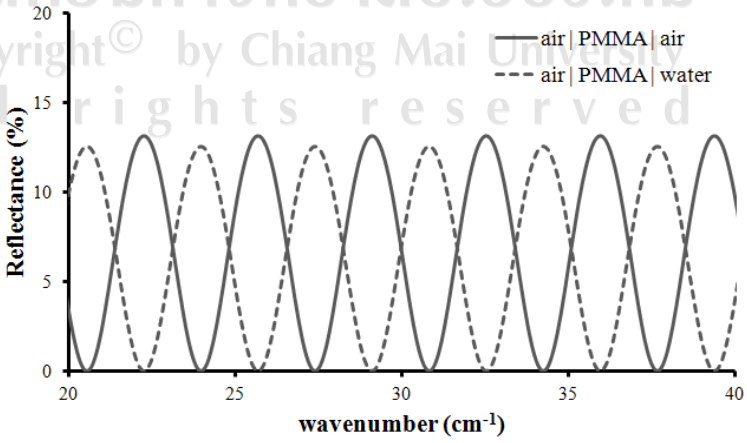

Figure 2.9: Spectral reflectance of the air|PMMA|air and air|PMMA|water structures.

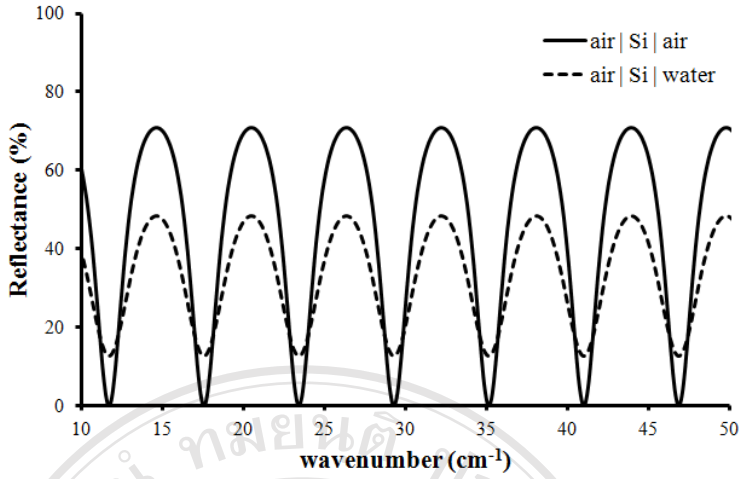

Figure 2.10: Spectral reflectance of the air|Si|air and air|Si|water structures.

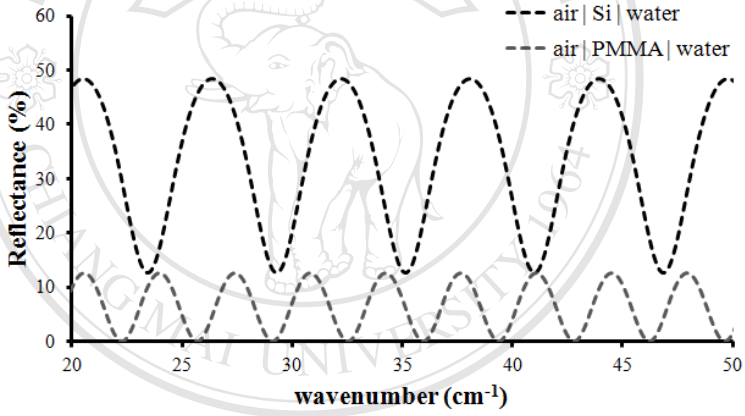

Figure 2.11: Spectral reflectance of the air|Si|water and air|PMMA|water structures.

2.4 Frequency Selection by Filter

Metal mesh filter is one of radio-frequency filtering methods to select frequency band in the electromagnetic waves. It was first used in far infrared and sub millimeter wave instrument by Ulrich [18]. This work found that an electromagnetic wave incident on the metal mesh structure gives rise to electromagnetic induction as the field induced surface currents flow in the closed loops of mesh. At the same time, charge distribution varies in time depending on the field amplitude, phase, and polarization. The optical transmission properties of metal grids have to be dependent only on the geometric properties of mesh. In the literature, one of the methods used to

predict the selected frequency by metal mesh is based on the transmission line theory. An equivalent circuit representation is employed as a simple model to describe the optical properties of the metal grid. A typical structure of mesh is the inductive grid shown in Figure 2.12. The inset of Figure shows an equivalent circuit to the inductive grid.

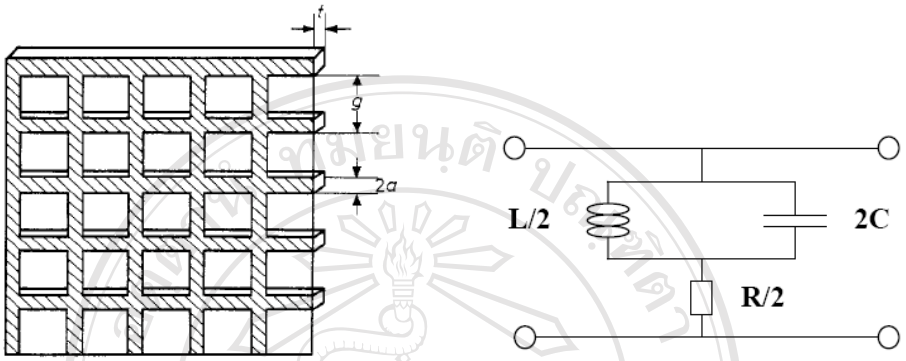

Figure 2.12: Inductive mesh geometry and its equivalent circuit [19].

We can express the relation between the loss resistance *(R)*, the inductance *(L)*, the capacitance *(C)*, the transmission of this circuit and the dimensions of the grid as [19]:

$$R = \frac{g}{4a}\left(\frac{c\omega_0}{g\sigma}\right)^{1/2} \tag{2.23}$$

$$L = \frac{Z_0}{\omega_0} \tag{2.24}$$

$$C = \frac{1}{Z_0\omega_0} \tag{2.25}$$

$$|T(\omega)|^2 = \frac{R^2+Z_0^2/\Omega^2}{(1+R)^2+Z_0^2/\Omega^2} \tag{2.26}$$

where c is speed of light, σ is the conductivity, Ω is generalized frequency that is equal to $\omega/\omega_0 - \omega_0/\omega$, ω_0 is the resonant frequency is equal to $1 - 0.27(a/g)$ and $Z_0 = 2\ln\csc(a\pi/2g)$ is the normalized impedance of L and C at resonance.

Two different dimensions of opening of grid mesh structures have been examined in an effort to better control the transmission band structure. They are

mesh-40 and mesh-80, see their profiles in Table 2.2. The transmission spectra of the three filters are computed by using the equivalent circuit method and shown in Figure 2.13. The frequencies of the pass band are mainly determined by the length of the opening size. From Figure 2.13, we can achieve the pass band at full width half maximum for each filter in the followings: 10 - 22 cm^{-1} for mesh-40, and 18 - 54 cm^{-1} for mesh-80.

Table 2.2: Geometry of copper meshes.

	Mesh-40	Mesh-80
Mesh	40 x 40 per inch	80 x 80 per inch
Wire diameter	0.2540 mm	0.1397 mm
Opening size	0.38 mm	0.18 mm
Open area percentage	36%	31%
Thickness	0.5080 mm	0.2794 mm
Weight per square meter	1.51 Kg	0.93 Kg

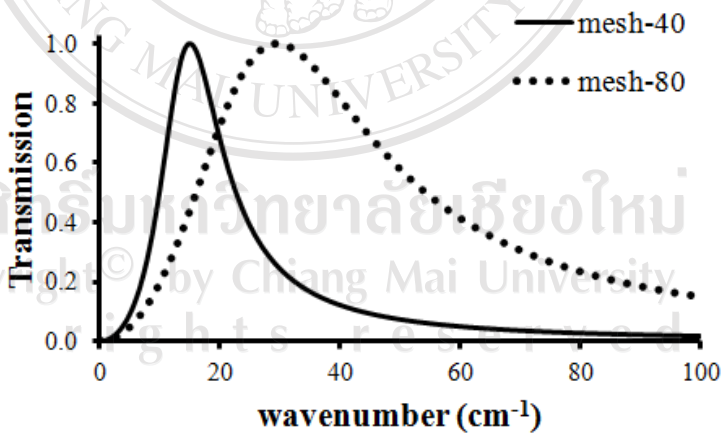

Figure 2.13: Transmission spectra of THz radiation obtain from the equivalent circuit method.

The theoretical framework, provided in this Chapter, will be helpful towards understanding THz measurement in Chapter 4. The calculation of THz response to the PEM fuel cell structure as well as the transmission band of THz using mesh filter ensure the potential applications of THz imaging to study water distribution in the PEM fuel cells.